Solar Panel Mains Inverter with Improved Efficiency

Conference Paper · September 2018

DOI: 10.1109/UPEC.2018.8542116

6 authors, including:

Chi-Thang Phan-Tan
Cork Institute of Technology

Nam Nguyen-Quang
Ho Chi Minh City University of Technology (HCMUT)

Noel Barry
Cork Institute of Technology

Martin Hill
Cork Institute of Technology

Solar Panel Mains Inverter with Improved Efficiency

Chi-Thang Phan-Tan[1,2], Nam Nguyen-Quang[2], Joe Connell[1], Noel Barry[1], Colin Levis[1], Martin Hill[1]
Department of Electrical & Electronic Engineering
[1] Cork Institute of Technology, Cork, Ireland
[2] Ho Chi Minh City University of Technology, Ho Chi Minh City, Vietnam
chi.phan-tan@mycit.ie

***Abstract*—A photovoltaic (PV) 2-stage micro-inverter is introduced with a separate DC/DC converter and DC/AC inverter. These two parts are connected by a DC-link that incorporates a low voltage energy buffer that is suitable for operation with a capacitor or low voltage battery. A novel maximum power point tracking (MPPT) method is applied to the DC/DC converter with improved efficiency and stability. The topology of the DC/AC converter is developed with the goal of reducing cost and device size. The converter design is developed with an integrated PWM high-frequency (20kHz) transformer to boost voltage to grid level before smoothing with an LC filter for 50Hz output. Experimental results of the MPPT efficiency and the DC/AC topology are presented to verify operation.**

Keywords—photovoltaic, micro-inverter, MPPT

I. Introduction

The purpose of this work is to design a micro-inverter that can integrate a low wattage battery as energy storage. The inverter should maximize its input through MPPT (maximum power point tracking) algorithm and its output should be 50Hz AC at grid level.

A micro-inverter is a DC/AC converter which is used for a single photovoltaic (PV) panel. The micro-inverter is proved better than string inverter for its efficiency under shaded conditions. Micro-inverters also perform better than string inverters in production, roof utilization, safety, installation and maintenance [1]-[3]. However, the inverter price, monitoring cost and payback time of a system using micro-inverters are higher than a system using string inverters [3].

The topology is able to apply a battery as an energy buffer. With a high penetration PV system, reverse power flow from the PV panels to the grid can cause over-voltage issues. The battery can balance the input and output of the inverter by storing or supplying energy to regulate and support the grid [4]-[6]. It also reduces the electricity bill by optimizing the energy exporting to the grid [7]. These features of the battery are necessary for smart inverters in micro-grid applications.

In a PV application, the plant efficiency in capturing available solar energy is principally determined by the MPPT algorithm. The output power of a solar panel depends on its I-V characteristic curve, temperature and irradiation. Moreover, the unstable components of the environment such as clouds or shading objects make the operating point of the solar panel change frequently. Therefore, the MPPT algorithm needs to make the system adapt quickly to the environment. There are many MPPT methods such as Perturb-and-Observed (P&O), Incremental-Conductance, Fuzzy-Logic and Artificial-Neural-Network. Some of these methods are complex and some are simple [8]-[12]. In this paper, a simple and effective MPPT is introduced.

The detailed description of the inverter is explained in the theory and simulation. The verification for the theory is shown in the experimental results.

II. Theory and Simulation

A. Overview

The requirements for this micro-inverter are the ability to integrate a battery and operate from a single PV panel. For a string-inverter, the input is a group of PV panels connected in series where the voltage is at a high level of up to 600V. Hence, the string inverter does not need to boost the voltage to grid level. On the other hand, the maximum output voltage of a single PV panel is around 40V, this means the micro-inverter needs a transformer for increasing the voltage to grid level. In addition, the battery to be integrated into the inverter should have small capacity and this results in a DC-link low voltage value. The DC-link voltage needs to be equal or higher than the input voltage. For example, a typical Li-ion cell is 3.7V, so that to have a higher voltage, the battery cells need to be connected in series. The reasonable number of the battery is around ten cells or 37V which both makes the voltage higher and keeps the size suitable for a micro-inverter. For those reasons, a proposed 2-stage inverter is introduced in Fig. 1.

The first stage of the micro-inverter is the DC/DC converter which is a SEPIC (single-ended primary-inductor converter). This converter is controlled by a novel MPPT algorithm for finding the maximum power point (MPP).

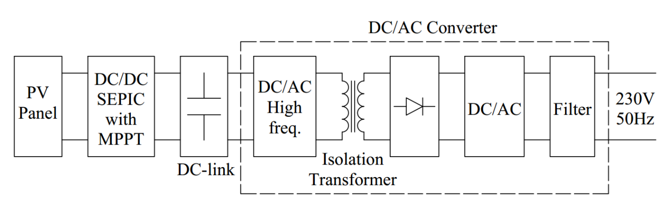

Fig. 1. Block diagram of micro-inverter

The second stage of the inverter is the DC/AC converter. This converter can convert DC from a low level to AC at grid level. It can be obtained by using an isolating high frequency transformer to boost the voltage to a higher level.

Between the DC/DC and DC/AC converter, there is a DC-link which can be realized with capacitors and/or a battery. In this work, the DC/DC and DC/AC converters are developed independently and are introduced in the following sections.

B. DC/DC converter with improved MPPT

The DC/DC converter chosen in this application is SEPIC. It is a buck-boost DC/DC converter which is necessary when integrating a battery at the DC-link. Its input current is continuous and its output has the same polarity as the input. The SEPIC is controlled by applying a duty cycle to a switch as shown in Fig. 2.

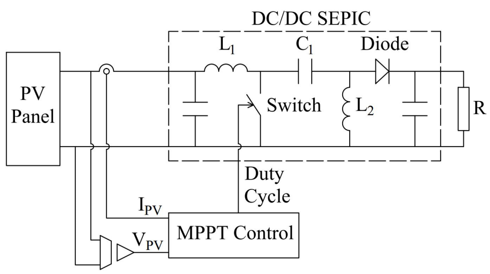

Fig. 2. DC/DC SEPIC schematic and MPPT control

To obtain maximum power, the PV current and voltage are measured and then the MPPT algorithm assigns the duty cycle to the switch of the DC/DC converter. A novel and simple MPPT method is developed called BS-P&O which combines the traditional P&O and binary-searching (BS) methods. The flowchart of the BS-P&O algorithm is shown in Fig. 3. The duty cycle D is used for controlling the SEPIC.

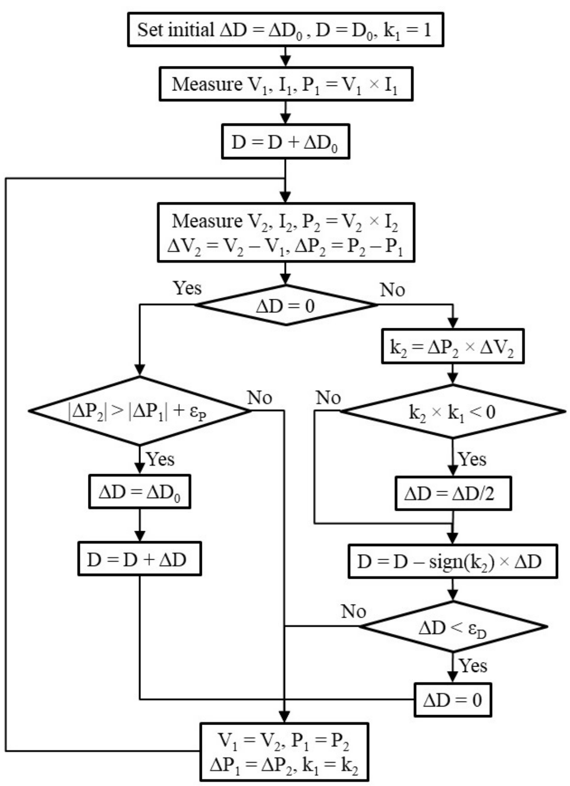

Fig. 3. Flowchart of BS-P&O theory

The PV voltage is controlled by increasing or decreasing by an increment of ΔD. In the beginning, a large ΔD is used to make the operating power point move quickly to the vicinity of the MPP. In Fig. 4, it can be seen that $\Delta P \times \Delta V$ is negative when the operating point is at the right side of the MPP and vice versa. Therefore, every time the value $\Delta P \times \Delta V$ changes its sign, the MPP must be between the two latest operating points and as the algorithm is approaching closer to the MPP, the change of duty cycle ΔD will be divided by a factor of two.

While ΔD equals zero and if there is any change of environment making the value of ΔP larger than the previous one, the algorithm will immediately set ΔD to ΔD_0 and start to search for the next MPP. The value of ε_P is added to compensate for the unwanted fluctuation of the measurement. As seen in the flowchart in Fig. 3, the smaller the duty cycle increment ΔD value, the closer the operating point to the MPP. In theory, the ΔD can be divided by two forever, however, the calculation in both simulation and programming has its limit. So that when the ΔD becomes too small and less than ε_D, the value of ΔD is set zero.

This simple method helps the converter converge close to MPP at an exponential rate. The illustration for this method is shown in Fig. 4.

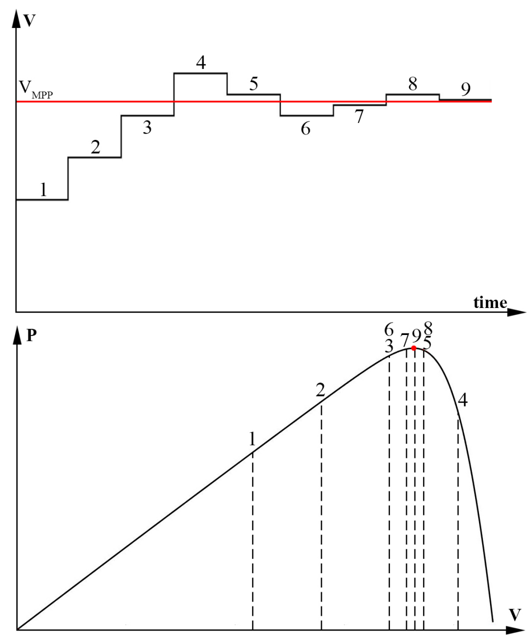

Fig. 4. Illustration of BS-P&O method

A simulation, using ideal components and measurements, of the BS-P&O system response to a step change in incident irradiation is shown in Fig. 5. The performance of an MPPT algorithm is characterized by the efficiency and time response to changes in the environment. In the simulation, the irradiation is constant for the first 0.4s, and then it is dropped to a lower value for the next 0.4s after which it returns to its initial value.

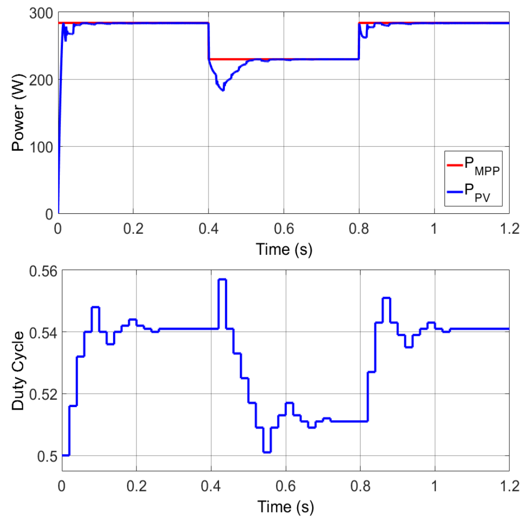

Fig. 5. Simulation of the BS-P&O

The simulated steady-state efficiency of the BS-P&O is 99.9% and the time response is less than 0.15s. This proves that the BS-P&O method is suitable for PV applications with high efficiency and quick time response.

C. *DC/AC converter*

Based on DC/AC topologies which apply a high frequency transformer in [13][14], the topology of the DC/AC converter is shown in Fig. 6. The challenge of designing this converter is that the DC input voltage is at a low level while the output is at grid level. Therefore a transformer is needed to boost the voltage. It is known that the higher the frequency, the smaller the transformer's size and vice versa. If the transformer is placed after the converter, the Sine Pulse-Width-Modulation (SPWM) waveform can be easily created by an H-bridge from the DC input. Then the SPWM is filtered to 50Hz and passes through the transformer. This makes the size of the transformer large and is not suitable for a micro-inverter. Therefore, an alternative approach is applied to the high-frequency transformer as shown in Fig. 6.

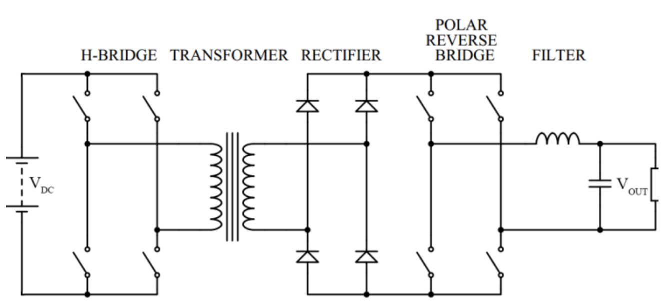

Fig. 6. DC/AC converter schematic

The first stage is an H-bridge, which creates the high frequency PWM pulses. These pulses then pass through a transformer to boost the voltage to grid level. After that, a diode rectifier bridge is used to flip all pulses in negative side to positive side. There is no need to have an active rectifier because the current does not flow backwards and the control is much simpler with the diode rectifier in comparison to an active switched rectifier. The next stage of the inverter is the polar reverse bridge to flip pulses at the frequency of 50Hz. And the final stage is an LC filter which blocks all high frequency components and just lets the fundamental frequency signal, 50Hz sinusoidal wave, pass through. The passive LC filter is selected for its simplicity and it does not need to be controlled by the microcontroller. The illustration of the waveform at stages of the DC/AC topology is shown in Fig. 7.

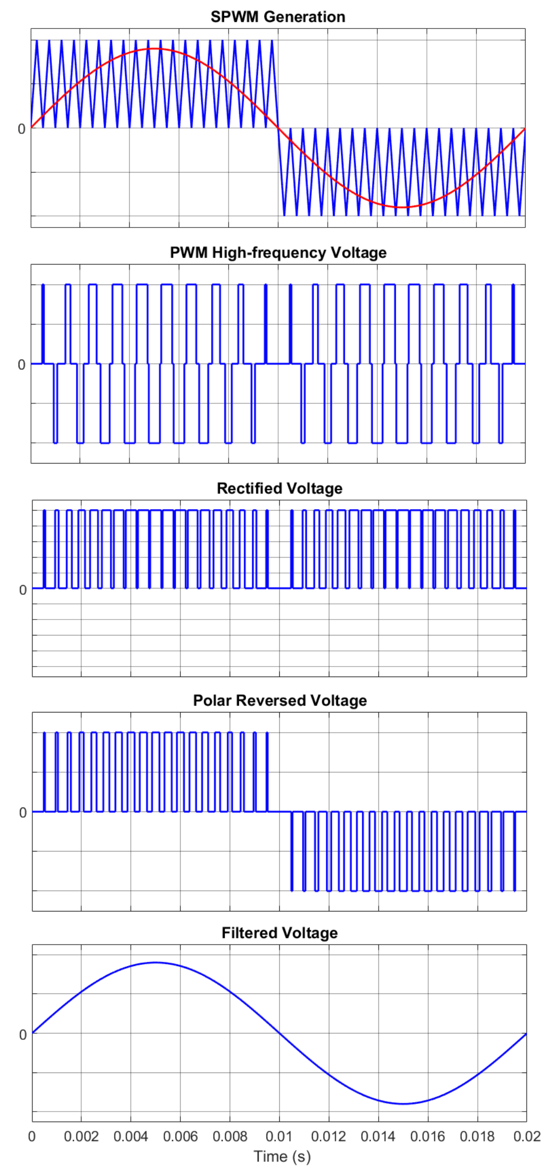

Fig. 7. Illustration of DC/AC waveform

The theory and simulation of the MPPT method and DC/AC converter topology are represented. The experiment results are shown in the next section.

III. Experimental Results

To verify the theory and simulation of the DC/DC MPPT algorithm and DC/AC topology, circuit boards were built to collect experimental results.

A. *DC/DC circuit with improved MPPT*

The DC/DC SEPIC circuit is shown in Fig. 10. The SEPIC has two inductors of 0.28mH, the capacitor in between is polypropylene of 10µF.

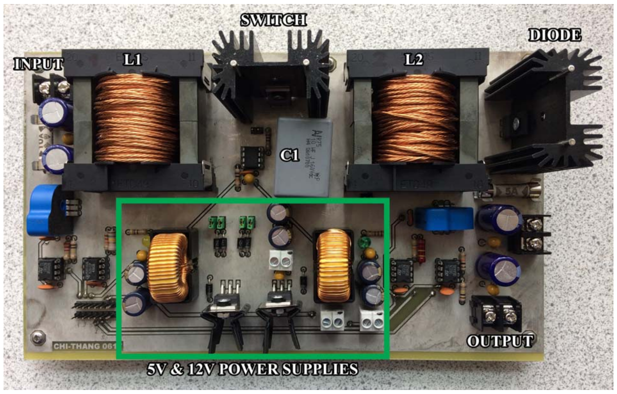

Fig. 8. DC/DC SEPIC prototype (*The labels are as shown in Fig. 2*)

In this test, the solar module is initially set to reach the MPP. After that, it is partially covered for about one second and then uncovered for the rest of time. By doing this, the response time of the algorithm under sudden changes in the environment is measured.

As it can be seen in Fig. 9 that the PV power drops quickly due to the change in irradiance, and then it soon moves to the new point. The change in duty cycle and the voltage are large in the transition and become smaller to get closer to the MPP.

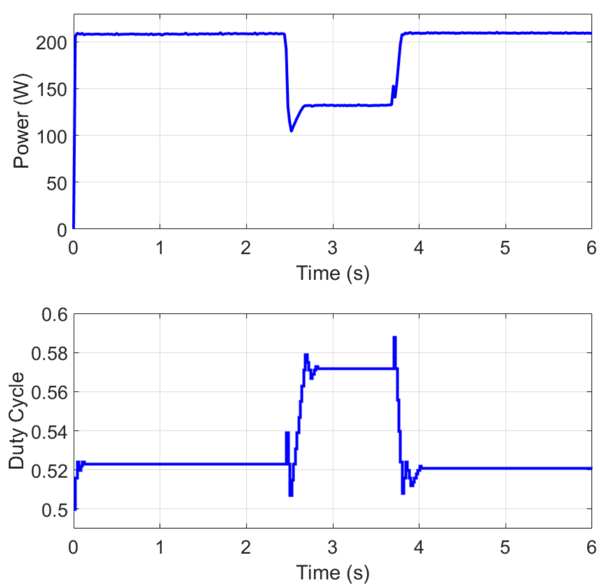

Fig. 9. Experimental results of BS-P&O

The steady-state efficiency of the experiment is measured at 99.23% and the response time of this algorithm is less than 0.2s, which is similar to the simulation and proves its effectiveness.

B. *DC/AC circuit*

A laboratory prototype of the DC/AC circuit is shown in Fig. 10. The transformer and the filtering inductor were manually wound.

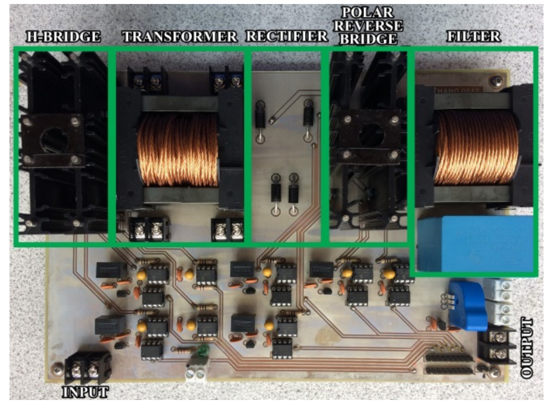

Fig. 10. DC/AC converter prototype (*The labels are as shown in Fig. 6*)

In the experiment, the converter is set up as seen in Fig. 6. The input of the converter is connected to a DC source and its output is connected to a resistor. The frequency passing through the transformer is 20kHz.

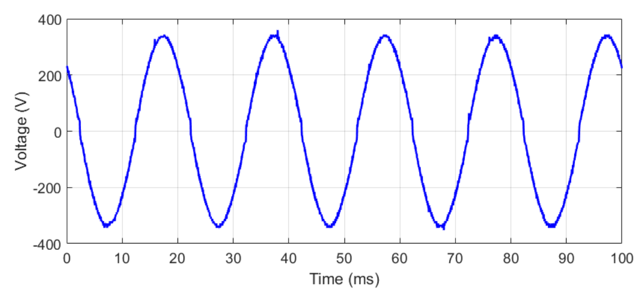

Fig. 11. Experimental result of DC/AC output

The measured output voltage of the DC/AC converter is shown in Fig. 11. The input of the converter is 30VDC and its output voltage is 230VAC at 50Hz. The total harmonic distortion (THD) is calculated as 3.83% which is less than 5% as required in IEEE 519-1992 standard.

IV. Conclusion

In this work, a 2-stage micro-inverter is introduced and verified by both the simulation and experiment. The first stage was a DC/DC SEPIC converter with a novel MPPT algorithm. The BS-P&O method performed with high efficiency (99.23%) and a quick response (<0.2s) to changes in the environment.

The second stage is the DC/AC topology which was designed to boost a low DC voltage to AC at the grid level of 230VAC and frequency of 50Hz. This topology has the advantage of using a high-frequency PWM transformer which makes the transformer's size small. The topology is introduced and verified by a hardware circuit.

The proposed micro-inverter has potentially wide applications for energy balancing and micro-grid control. Future developments will include energy balancing using a battery buffer and controlled power delivery to a grid-connection.

References

[1] F. Famoso, R. Lanzafame, S. Maenza, and P. F. Scandura, "Performance Comparison between Micro-inverter and String-inverter Photovoltaic Systems," *Energy Procedia*, vol. 81, pp. 526– 539, Dec. 2015.

[2] S. Strache, R. Wunderlich and S. Heinen, "A Comprehensive, Quantitative Comparison of Inverter Architectures for Various PV Systems, PV Cells, and Irradiance Profiles," in *IEEE Transactions on Sustainable Energy*, vol. 5, no. 3, pp. 813-822, July 2014.

[3] O. A. Arráez-Cancelliere, N. Muñoz-Galeano and J. M. Lopez-Lezama, "Performance and economical comparison between micro-inverter and string inverter in a 5, 1 kWp residential PV-system in Colombia," *2017 IEEE Workshop on Power Electronics and Power Quality Applications (PEPQA)*, Bogota, 2017, pp. 1-5.

[4] M. P. Behera, P. K. Ray and G. H. Beng, "Single-phase grid-tied photovoltaic inverter to control active and reactive power with battery energy storage device," *2016 IEEE Region 10 Conference (TENCON)*, Singapore, 2016, pp. 1900-1904.

[5] J. Khajesalehi, K. Sheshyekani, M. Hamzeh and E. Afjei, "High-performance hybrid photovoltaic -battery system based on quasi-Z-source inverter: application in microgrids," in *IET Generation, Transmission & Distribution*, vol. 9, no. 10, pp. 895-902, 7 2 2015.

[6] C. L. Nge, O. M. Midtgård and L. Norum, "Energy efficiency analysis of grid-connected photovoltaic inverter with storage battery," *Proceedings of the 2011 14th European Conference on Power Electronics and Applications*, Birmingham, 2011, pp. 1-10.

[7] Riffonneau, Y., Bacha, S., Barruel, F., Ploix, S.: "Optimal power flow management for grid-connected PV systems with batteries", *IEEE Trans. Sustain. Energy*, 2011, pp. 309 –320.

[8] B. Subudhi and R. Pradhan, "A Comparative Study on Maximum Power Point Tracking Techniques for Photovoltaic Power Systems," in *IEEE Transactions on Sustainable Energy*, vol. 4, no. 1, pp. 89-98, Jan. 2013.

[9] T. Esram and P. L. Chapman, "Comparison of Photovoltaic Array Maximum Power Point Tracking Techniques," in *IEEE Transactions on Energy Conversion*, vol. 22, no. 2, pp. 439-449, June 2007.

[10] R. Faranda, S. Leva and V. Maugeri, "MPPT techniques for PV Systems: Energetic and cost comparison," *2008 IEEE Power and Energy Society General Meeting - Conversion and Delivery of Electrical Energy in the 21st Century*, Pittsburgh, PA, 2008, pp. 1-6.

[11] M. A. Elgendy, B. Zahawi and D. J. Atkinson, "Dynamic behaviour of hill-climbing MPPT algorithms at low perturbation rates," *IET Conference on Renewable Power Generation (RPG 2011)*, Edinburgh, 2011, pp. 1-6.

[12] L. Zhang, W. G. Hurley and W. H. Wölfle, "A New Approach to Achieve Maximum Power Point Tracking for PV System With a Variable Inductor," in *IEEE Transactions on Power Electronics*, vol. 26, no. 4, pp. 1031-1037, April 2011.

[13] M. Z. Ramli, Z. Salam, Leong Soon Toh and Chee Lim Nge, "A bidirectional high-frequency link inverter using center-tapped transformer," *2004 IEEE 35th Annual Power Electronics Specialists Conference (IEEE Cat. No.04CH37551)*, 2004, pp. 3883-3888 Vol.5.

[14] E. Koutroulis, J. Chatzakis, K. Kalaitzakis and N. C. Voulgaris, "A bidirectional, sinusoidal, high-frequency inverter design," in *IEE Proceedings - Electric Power Applications*, vol. 148, no. 4, pp. 315-321, Jul 2001.